Journal of Solid Mechanics Vol. 13, No. 1 (2021) pp. 95-113
DOI: 10.22034/jsm.2020.1906422.1632

Vibrations of Inhomogeneous Visco thermoelastic Nonlocal Hollow Sphere under the effect of Three-Phase-Lag Model

S.R. Sharma [1], M.K. Sharma [2], D.K. Sharma [2,*]

[1]*Chitkara University School of Engineering and Technology, Chitkara University, Himachal Pradesh, 174103, India*
[2]*Department of Mathematics, Maharaja Agrasen University, Baddi Solan, 174103, India*

Received 8 December 2020; accepted 26 January 2021

ABSTRACT

Herein, the free vibrations of inhomogeneous nonlocal visco thermoelastic sphere with three-phase-lag model of generalized thermoelasticity have been addressed. The governing equations and constitutive relations with three-phase-lag model have been solved by using non-dimensional quantities. The simple power law has been presumed to take the material in radial direction. The series solution has been established to derive the solution analytically. The relations of frequency equations for the continuation of viable modes are developed in dense form. The analytical results have been authenticated by the reduction of nonlocal and three–phase–lag parameters. To investigate the quality of vibrations, frequency equations are determined by applying the numerical iteration method. MATLAB software tools have been used for numerical computations and simulations to present the results graphically subject to natural frequencies, frequency shift, and thermoelastic damping. The numerical results clearly show that the variation of vibrations is slightly larger in case of nonlocal elastic sphere in contrast to elastic sphere.

Keywords: Functionally graded material; Nonlocal elasticity; Three-phase-lag model; Vibrations; Frequency shift, Dual–phase–lag model.

1 INTRODUCTION

THE theories of linear thermo-elasticity were established by Nowacki [1] thoroughly. Lord and Shulman (LS) [2], Green and Lindsay (GL) [3], Green and Naghdi (GN) [4] and more authors developed the theories of generalized thermoelasticity. After a span of time, a dual-phase-lag (DPL) heat conduction model which includes the effect of microscopic interactions was developed by Chandrasekharaiah [5] and Tzou [6]. Roy Choudhuri [7] derived another thermoelastic model based on three-phase-lag (TPL) model of heat conduction in the context of generalized thermoelasticity. In this model, three different phase–lags, namely τ_q , τ_T and τ_υ have been considered in the classical Fourier's law: $\vec{q} = -K\vec{\nabla}T$ as $\vec{q}(P,t+\tau_q) = -\left[K\vec{\nabla}T(P,t+\tau_T) + K^*\vec{\nabla}\upsilon(P,t+\tau_\upsilon)\right]$, where K^*,

*Corresponding author.
E-mail address: dksharma200513@gmail.com (D.K.Sharma)

$\vec{\nabla}\upsilon$ and τ_{υ} are additional material constant, thermal displacement gradient and phase-lag of thermal displacement gradient respectively. TPL model has importance in exploring various applications related to nuclear boiling, electron phonon interactions, scattering, etc. Some of the applications of the DPL and TPL models might be initiated in ref. [8-10].

In mechanical point of view, the elasticity in the context of non-locality was explored by Eringen [11]. He addressed a unique foundation for the improvement of basic field equations for the continuation of continuum nonlocal elastic theories. Moreover, in this model which was based on the theory of non-locality, the applied stress at a specific point of continuum elastic body does not only depend upon the strain at that particular point, but also at all other surrounding points of the strain of the body. The theories of elasticity in the context of non-locality have been employed to the propagation of a plane wave in the context of classical and non-classical theories. A few researchers of such works are Ghadiri et al. [12], Li et al. [13], Zarei et al. [14], Najafizadeh et al. [15] etc. Bachher and Sarkar [16] investigated a nonlocal thermoelasticity theory for the fractional derivative of heat transfer with voids. Mondal et al. [17] explored the nonlocal thermoelastic waves in the DPL model with voids material. Asbaghian Namin and Pilafkan [18] investigated the influences of boundary conditions and small scale effect on the vibrations of nano-plates in the context of classical theory. Elastic nonlocal thermoelasticity of type II was thoroughly investigated by Sarkar et al. [19]. Othman et al. [20-21] studied the visco thermoelastic waves and the effect of magnetic field on thermoelasticity theories with two temperatures. Soltani et al. [22] studied the vibrations of single walled fluid filled nanotube in the context of nonlocal theory of elasticity. Marin et al. [23] studied the mixed initial value problems for porous bodies in the context of micropolar continuum mechanics. The initial studies on vibrating spheres were explored by Lamb [24], Sato and Usami [25, 26], etc. The coupling between elastic and thermal fields for spheres and cylinders were explored by Hsu [27], Keles and Tutuncu [28], Sharma et al. [29-31], Nejad et al. [32], Sharma [33], Biswas and Mukhopadhyay [34], Biswas [35], Sharma et al. [36-37], Manthena et al. [38–39], Sharma and Mittal [40], etc. Riaz et al. [41] investigated the effect of heat transfer on Eyring Powell fluid model through a rectangular channel. Bhatti et al. [42] explored the numerical study of Hall current impact and heat transfer on the propulsion of fluid particle suspended with wall properties. In the reference of LS model, Sharma et al. [43–44] conducted an analysis of stress free vibrations by considering nonlocal elastic hollow cylinder with void and diffusion. Biswas [45] expressed equations of steady oscillations in the context of nonlocal thermoelastic medium with the voids material. Pramanik and Biswas [46] presented the analysis of surface waves in the reference of nonlocal thermoelastic medium with a state space approach.

In current study, we represent free vibrations of three-phase-lag (TPL) model of isotropic functionally graded nonlocal visco thermoelastic sphere. The simple law of exponent has been assumed that the material is graded i.e. inhomogeneous in radial direction. The Fröbenious method [48, 50] of the power series is established to investigate the solution analytically. To discover the behavior of vibrations, the frequency relations are explained by employing numerical iteration method by using MATLAB software tools. The obtained analytical results have been presented graphically subject to natural frequencies, frequency shift, and quality factor related to thermoelastic damping to check the effects of different theories of thermoelasticity such as TPL, DPL, GN-III, LS and CTE. Using grading index parameter, tractions and vibrations may be managed by controlling the values of the index parameter as we need. The study may have applications that graded index parameter act as a regulator of variation of variations.

2 FORMULATION OF THE PROBLEM

2.1 The mathematical model

Here, we consider thermally conducting thermo-visco-elastic thick-walled sphere/disk of inner radius R_I and outer radius $R_O = \hbar R_I$, at uniform temperature T_0 initially in undisturbed state. Here the components of temperature and displacement in spherical coordinated system $(r,\ \theta,\ \phi)$ can be expressed as $T(r\ ,\ t)$ and $u_r = u(r,t)$, $u_\theta = u_\phi = 0$, respectively. The governing equations for isotropic inhomogeneous nonlocal visco thermoelastic sphere of inner, outer radii, R_I, $R_O = R_I\hbar$ respectively in the context of three-phase-lag model (TPL) [7] of generalized thermoelasticity with Eringen's nonlocal elasticity [11] (without heat sources and body forces) are:

2.1.1 Strain displacement relations

$$e_{\theta\theta} = e_{\phi\phi} = \frac{u}{r}\ ,\ e_{rr} = \frac{\partial u}{\partial r}, e_{r\theta} = e_{r\phi} = e_{\theta\phi} = 0 \tag{1}$$

2.1.2 Constitutive relations

$$\left.\begin{aligned}(1-\xi^2\nabla^2)\,\sigma_{rr} = \sigma_{rr}^L = (\lambda+2\mu)e_{rr} + \lambda e_{\theta\theta} - \beta^* T \\ (1-\xi^2\nabla^2)\,\sigma_{\theta\theta} = \sigma_{\theta\theta}^L = 2(\lambda+\mu)e_{\theta\theta} + \lambda e_{rr} - \beta^* T\end{aligned}\right\} \tag{2}$$

2.1.3 Equation of motion

$$\frac{\partial \sigma_{rr}^L}{\partial r} + \frac{2\,(\sigma_{rr}^L - \sigma_{\theta\theta}^L)}{r} = \rho(1-\xi^2\nabla^2)\frac{\partial u}{\partial t} \tag{3}$$

2.1.4 Equation of heat conduction

$$\left(1 + t_q\,\frac{\partial}{\partial t} + \frac{1}{2}t_q^2\,\frac{\partial^2}{\partial t^2}\right)\left(\rho C_e\,\frac{\partial^2 T}{\partial t^2} + \beta^* T_0\,\frac{\partial^2 e}{\partial t^2}\right) = \left(K^* + t_\nu^*\,\frac{\partial}{\partial t} + K\ t_T\,\frac{\partial^2}{\partial t^2}\right)\nabla^2 T \tag{4}$$

where the superscript 'L' in stresses denotes local elasticity; e is the cubical dilatation.

Here $e = e_{rr} + e_{\theta\theta} + e_{\phi\phi}$, $t_\nu^* = K + t_\nu K^*$, $\nabla^2 = \dfrac{\partial^2}{\partial r^2} + \dfrac{2}{r}\dfrac{\partial}{\partial r}$, $\sigma_{ij}^L = \sigma_{ij}$; i , $j = r$, θ . Note that Eq. (4) reduces to different theories of generalized visco thermoelastic ity as below:

I. *TPL* model: $t_T \neq 0, t_\nu \neq 0, t_q \neq 0$.

II. *DPL* model: $t_T \neq 0, t_\nu = 0, t_q \neq 0$, $K^* = 0$.

III. *GN III* model: $t_T = t_\nu = t_q = 0$.

IV. *LS* model: $t_T = t_\nu = t_q^2 = 0, t_q = t_0 > 0$, $K^* = 0$.

Here, the material has been considered to be isotropic and graded due to simple power law as reported in Sharma et al. [31] in such a way that

$$\left(\lambda\,,\ \mu\,,\ \beta^*\,,\ \rho\,,\ K\,,\ K^*\right) = \left(\lambda_0\,,\ \mu_0\,,\ \beta_0^*\,,\ \rho_e\,,\ K_0\,,\ K_0^*\right)\left(\frac{r}{R_I}\right)^\alpha \tag{5}$$

Here the exponent α denotes the degree of in-homogeneity. The parameters λ_0 , μ_0 , β_0^* , ρ_e , K_0 , K_0^* are homogenous corresponding items of the respective quantities. Noda and Jin [47] observed that in comparison to thermal conductivity and elastic modulus, the linear thermal expansion coefficients are not significant contributors and therefore must be considered as homogenous (constant). For the visco thermoelastic sphere, the material parameters are defined in the following manner $\lambda_0 = \lambda_e\left(1 + \alpha_0\,\dfrac{\partial}{\partial t}\right)$, $\mu_0 = \mu_e\left(1 + \alpha_1\,\dfrac{\partial}{\partial t}\right)$, $\beta_0^* = \beta_e\left(1 + \beta_0\,\dfrac{\partial}{\partial t}\right)$, where $\beta_e = (3\lambda_e + 2\mu_e)\,\alpha_T$ and $\beta_0 = \dfrac{(3\lambda_e\alpha_0 + 2\mu_e\alpha_1)\,\alpha_T}{\beta_e}$. The quantities λ_e , μ_e are well known Lame's parameters, α_0 , α_1 are the mechanical relaxation time parameters. Solving Eqs. (3) and (4) by using Eqs. (1), (2) and (5), for the unknown radial displacement and temperature, we obtain the following equations:

$$\frac{\rho_e}{(\lambda_e+2\mu_e)}(1-\xi^2\nabla_m^2)\ddot{u}=\left(1+\delta_0\frac{\partial}{\partial t}\right)\nabla_m^2 u+\frac{m_2^*}{r^2}u-\frac{\beta_e}{(\lambda_e+2\mu_e)}\left(1+\beta_0\frac{\partial}{\partial t}\right)\left(\frac{\partial T}{\partial r}+\frac{\alpha}{r}T\right) \tag{6}$$

$$\frac{\partial^2}{\partial t^2}\left(1+t_q\frac{\partial}{\partial t}+\frac{t_q^2}{2}\frac{\partial^2}{\partial t^2}\right)\left(\rho C_e T+\beta_e T_0\left(1+\beta_0\frac{\partial}{\partial t}\right)e\right)=\left(K_0\left(\frac{\partial}{\partial t}+t_T\frac{\partial^2}{\partial t^2}\right)+K_0^*\left(1+t_\nu\frac{\partial}{\partial t}\right)\right)\nabla_m^2 T \tag{7}$$

where $m_1=\alpha+2,\ m_2^*=2\left[\lambda_0(\alpha-1)-2\mu_0\right],\nabla_m^2=\dfrac{\partial^2}{\partial r^2}+\dfrac{m_1}{r}\dfrac{\partial}{\partial r}$.

2.2 Regular and initial boundary conditions

It is believed that the generalized inhomogeneous nonlocal visco thermoelastic sphere is initially undisturbed and rest position, hence initial boundary conditions are:

$$T(r,0)=0=\frac{\partial T(r,0)}{\partial t},\ u(r,0)=0=\frac{\partial u(r,0)}{\partial t},\ \sigma_{rr}(r,0)=0 \text{ at } \quad r=R_I \quad , \quad \hbar R_I \tag{8}$$

The analysis is conducted on the surface of the sphere by considering traction free, thermal boundary conditions at the inner, outer radii $r=R_I$, $R_O=R_I\,\hbar$ respectively. Mathematically, there are two sets of boundary conditions as given below:

For traction-free thermally insulated surfaces of the sphere, we have

$$\frac{\partial T}{\partial r}=0\ ;\sigma_{rr}=0 \quad \text{at} \quad r=R_I,\ \hbar R_I \tag{9}$$

For traction-free isothermal surfaces of the sphere, we have

$$T=0\ ;\ \sigma_{rr}=0 \quad \text{at} \quad r=R_I,\ \hbar R_I \tag{10}$$

3 METHODOLOGIES

3.1 Solution of the model

Non-dimensional parameters are introduced as:

$$\begin{cases}(\tau_q,\tau_T,\tau_\nu,\tau)=\dfrac{c_1}{R_I}(t_q,t_T,t_\nu,t),\ \ \delta_0=\hat{\alpha}_0+2\delta^2(\hat{\alpha}_1-\hat{\alpha}_0),\ \Theta=\dfrac{T}{T_0},\\ (w,r,\xi_0)=\dfrac{1}{R_I}(u,r,\xi),\ \bar{\varepsilon}=\dfrac{\beta_e T_0}{(\lambda_e+2\mu_e)},\ (\hat{\alpha}_0,\hat{\alpha}_1,\hat{\beta}_0)=\dfrac{c_1}{R_I}(\alpha_0,\alpha_1,\beta_0),\\ \delta^2=\dfrac{c_2^2}{c_1^2},\varepsilon_T=\dfrac{\beta_e^2 T_0}{\rho_e C_e(\lambda_e+2\mu_e)},\ \Omega^*=\dfrac{R_I\,\omega^*}{c_1},\ \tau_{RR}=\dfrac{\sigma_{rr}}{\rho_e c_1^2},\ \tau_{\Theta\Theta}=\dfrac{\sigma_{\theta\theta}}{\rho_e c_1^2},\end{cases} \tag{11}$$

Plugging the dimensionless quantities from Eqs. (11) in Eq. (2) and Eqs. (6) and (7), we obtain:

$$\left(1+\delta_0\frac{\partial}{\partial\tau}\right)\nabla_1^2 w+\frac{\hat{m}_2}{R^2}w-\bar{\varepsilon}\left(1+\hat{\beta}_0\frac{\partial}{\partial\tau}\right)\left(\frac{\partial\Theta}{\partial R}+\frac{\alpha}{R}\Theta\right)=(1-\xi_0^2\nabla_1^2)\frac{\partial^2 w}{\partial\tau^2} \tag{12}$$

$$\left(1+\tau_q\frac{\partial}{\partial\tau}+\frac{1}{2}\tau_q^2\frac{\partial^2}{\partial\tau^2}\right)\left[\Omega^*\frac{\partial^2\Theta}{\partial\tau^2}+\frac{\varepsilon_T\Omega^*}{\bar{\varepsilon}}\left(1+\hat{\beta}_0\frac{\partial}{\partial\tau}\right)\left(\frac{\partial}{\partial R}+\frac{2}{R}\right)\frac{\partial^2 w}{\partial\tau^2}\right]=\left\{\left(\frac{\partial}{\partial\tau}+\tau_T\frac{\partial^2}{\partial\tau^2}\right)+C_K^2\left(1+\tau_\nu\frac{\partial}{\partial\tau}\right)\right\}\nabla_1^2\Theta \tag{13}$$

$$\tau_{RR}^L=R^\alpha\left\{\left(1+\delta_0\frac{\partial}{\partial\tau}\right)\frac{\partial w}{\partial R}+2(1-2\delta^2)\left(1+\hat{\alpha}_0\frac{\partial}{\partial\tau}\right)\frac{w}{R}-\bar{\varepsilon}\left(1+\hat{\beta}_0\frac{\partial}{\partial\tau}\right)\Theta\right\} \tag{14}$$

$$\tau_{\theta\theta}^L=R^\alpha\left\{2(1-2\delta^2)\left(1+\hat{\alpha}_0\frac{\partial}{\partial\tau}\right)\left(\frac{\partial w}{\partial R}+\frac{w}{R}\right)+\left(1+\delta_0\frac{\partial}{\partial\tau}\right)\frac{w}{R}-\bar{\varepsilon}\left(1+\hat{\beta}_0\frac{\partial}{\partial\tau}\right)\Theta\right\} \tag{15}$$

where $C_K^2=\frac{R_I K_0^*}{c_1 K_0}$, $\hat{m}_2=2\left[\alpha(1-2\delta^2)\left(1+\hat{\alpha}_0\frac{\partial}{\partial\tau}\right)-\left(1+\delta_0\frac{\partial}{\partial\tau}\right)\right]$, $c_1^2=\frac{(\lambda_e+2\mu_e)}{\rho_e}$, $c_2^2=\frac{\mu_e}{\rho_e}$, $\omega^*=\frac{C_e(\lambda_e+2\mu_e)}{K_0}$, $\nabla_1^2=\frac{\partial^2}{\partial R^2}+\frac{m_1}{R}\frac{\partial}{\partial R}$.

3.2 Time harmonic vibrations

Here the time harmonic vibrations are presumed as:

$$\begin{pmatrix}w\\ \Theta\end{pmatrix}(R,\tau)=\begin{pmatrix}\bar{w}(R)\\ \bar{\Theta}(R)\end{pmatrix}e^{-i\,\Omega\tau} \tag{16}$$

where $\Omega=\frac{\omega R_I}{c_1}$ represents the circular frequency. Plugging the solution assumed from Eq. (16) in Eqs. (12) to (15), we get

$$\nabla_r^2\bar{w}+\left(\frac{m_2}{R^2}+\frac{i\,\Omega}{\tilde{\delta}_0^*}\right)\bar{w}-\frac{\bar{\varepsilon}\,\tilde{\beta}_0}{\tilde{\delta}_0^*}\left(\frac{d}{dR}+\frac{\alpha}{R}\right)\bar{\Theta}=0, \tag{17}$$

$$\nabla_r^2\bar{\Theta}+\Omega^*\Omega^3\tilde{\tau}_q\,\bar{\Theta}-im_4\Omega^4\,\tilde{\beta}_0\tilde{\tau}_q\left(\frac{d}{dR}+\frac{2}{R}\right)\bar{w}=0 \tag{18}$$

$$\tau_{RR}^L=-i\,\Omega\tilde{\delta}_0^* R^\alpha\left\{\frac{\partial\bar{w}}{\partial R}+2(1-2\delta^2)\frac{\tilde{\alpha}_0}{\tilde{\delta}_0}\frac{\bar{w}}{R}-\frac{\bar{\varepsilon}}{\tilde{\delta}_0}\tilde{\beta}_0\,\bar{\Theta}\right\}, \tag{19}$$

$$\tau_{\Theta\Theta}^L=-i\,\Omega\tilde{\delta}_0 R^\alpha\left\{2(1-2\delta^2)\frac{\tilde{\alpha}_0}{\tilde{\delta}_0}\left(\frac{\partial\bar{w}}{\partial R}+\frac{\bar{w}}{R}\right)+\frac{\bar{w}}{R}-\frac{\bar{\varepsilon}}{\tilde{\delta}_0}\tilde{\beta}_0\bar{\Theta}\right\} \tag{20}$$

where $m_2=2\left(\frac{\tilde{\alpha}_0(1-2\delta^2)\alpha-\tilde{\delta}_0}{\tilde{\delta}_0^*}\right)$, $\tilde{\delta}_0^*=\tilde{\delta}_0-i\,\Omega\xi_0^2$, $m_4=\frac{\varepsilon_T\Omega^*}{\bar{\varepsilon}}$, $\tilde{\delta}_0=\left(i\,\Omega^{-1}+\delta_0\right)$, $\tilde{\tau}_\nu=\tau_\nu+i\,\Omega^{-1}$, $\tilde{\tau}_T=\tau_T+i\,\Omega^{-1}$, $\tilde{\alpha}_0=\hat{\alpha}_0+i\,\Omega^{-1}$, $\tilde{\alpha}_1=\hat{\alpha}_1+i\,\Omega^{-1}$, $\tilde{\beta}_0=\hat{\beta}_0+i\,\Omega^{-1}$, $\tilde{\tau}_q=\frac{\left(i\,\Omega^{-2}+\tau_q\Omega^{-1}-\frac{1}{2}i\,\tau_q^2\right)}{\left(\tilde{\tau}_\nu C_K^2-i\,\Omega\tilde{\tau}_T\right)}$, $\nabla_r^2=\frac{d^2}{dR^2}+\frac{m_1}{R}\frac{d}{dR}$.

We now set up the transformation as already used by Sharma et al. [31]:

$$(\bar{w} \quad \bar{\Theta})(R) = (V(R) \quad \Psi(R))R^{-\frac{1+\alpha}{2}} \tag{21}$$

Thereafter, the transformation from Eq. (21) is used in Eqs. (17)–(20), which gives

$$\begin{cases} \nabla_R^2 V + \left(\dfrac{i\Omega}{\tilde{\delta}_0^*} - \dfrac{n^2}{R^2}\right)V - \dfrac{\bar{\varepsilon}\ \tilde{\beta}_0}{\tilde{\delta}_0^*}\left(\dfrac{d}{d\,R} - \dfrac{b^*}{R}\right)\Psi = 0, \\ \nabla_R^2\ \Psi + \left(\Omega^*\Omega^3\tilde{\tau}_q - \left(\dfrac{a^*}{R}\right)^2\right)\Psi - im_4\Omega^4\tilde{\beta}_0\tilde{\tau}_q\left(\dfrac{d}{d\,R} + \dfrac{(b^*+1)}{R}\right)V = 0, \end{cases} \tag{22}$$

$$\begin{cases} \tau_{RR}^L = -i\,\Omega\tilde{\delta}_0 R^{-a^*}\left\{\dfrac{\partial V}{\partial R} + h^*\dfrac{w}{R} - \dfrac{\bar{\varepsilon}}{\tilde{\delta}_0}\tilde{\beta}_0\,\Psi\right\}, \\ \tau_{\Theta\Theta}^L = -i\,\Omega\tilde{\delta}_0 R^{-a^*}\left\{2(1-2\delta^2)\dfrac{\tilde{\alpha}_0}{\tilde{\delta}_0}\dfrac{\partial V}{\partial R} + g^*\left(\dfrac{V}{R}\right) - \dfrac{\bar{\varepsilon}}{\tilde{\delta}_0}\tilde{\beta}_0\Psi\right\}, \end{cases} \tag{23}$$

where $n^2 = (a^*)^2 - m_2$, $a^* = \dfrac{1+\alpha}{2}$, $b^* = \dfrac{1-\alpha}{2}$, $h^* = \left(2(1-2\delta^2)\dfrac{\tilde{\alpha}_0}{\tilde{\delta}_0} - a^*\right)$, $\nabla_R^2 = \dfrac{1}{R}\dfrac{d}{dR}\left(R\dfrac{d}{dR}\right)$,

$g^* = \left(\dfrac{2(1-2\delta^2)\tilde{\alpha}_0 b^* + \tilde{\delta}_0}{\tilde{\delta}_0}\right)$.

3.3 Extended power series solution

From differential Eq. (22), it is noticed that $R = 0$ is regular singular point, and therefore the model is extended by using series solution as earlier presented by Tomantschger [48], hence we must have non–trivial solution given as:

$$\begin{pmatrix} V(R) \\ \Psi(R) \end{pmatrix} = \sum_{k=0}^{\infty}\begin{pmatrix} A_k \\ B_k \end{pmatrix}R^{s+k} \tag{24}$$

Here k is defined as Fröbenius parameter; the parameter s represents the eigenvalue (complex or real) and A_k , B_k represent the unknowns to be evaluated through the boundaries. Here the explanation for $R_I \le r \le \hbar R_I$, $R_I > 0$ is valid and therefore the domain for the system of differential Eqs. (22) is $1 \le R \le \hbar$. Substituting the solution (24) in the differential Eq. (22) and on simplification, we obtain

$$\sum_{k=0}^{\infty}\left\{\begin{pmatrix} a_{11} & 0 \\ 0 & a_{22} \end{pmatrix}\frac{1}{R^2} + \begin{pmatrix} 0 & a_{12} \\ a_{21} & 0 \end{pmatrix}\frac{1}{R} + \begin{pmatrix} h_{11} & 0 \\ 0 & h_{22} \end{pmatrix}\right\}\begin{pmatrix} A_k \\ B_k \end{pmatrix}R^{s+k} = 0 \tag{25}$$

where $a_{11} = (s+k)^2 - n^2$, $a_{21} = -B^*(s+k+b^*+1)$, $a_{22} = (s+k)^2 - (a^*)^2$, $a_{12} = A^*(s+k-b^*)$, $A^* = -\dfrac{\bar{\varepsilon}\ \tilde{\beta}_0}{\tilde{\delta}_0^*}$,

$B^* = im_4\Omega^4\tilde{\beta}_0\tilde{\tau}_q$, $h_{11} = i\,\Omega/\tilde{\delta}_0^*$, $h_{22} = \Omega^*\Omega^3\tilde{\tau}_q$.

Equating lowest power of coefficient of R ;$(i.e.\ R^{s-2})$ to zero in Eq. (25), we obtain:

$$\begin{pmatrix} s^2-n^2 & 0 \\ 0 & s^2-(a^*)^2 \end{pmatrix}\begin{pmatrix} A_0(s) \\ B_0(s) \end{pmatrix}=0 \tag{26}$$

The above homogenous Eq. (26) must have a non-trivial solution if and only if the determinant of matrix vanishes. The solution of Eq. (26) provide us the indicial equation whose roots are

$$s_1=n \quad , \quad s_2=-\,n \quad s_3=a^* \quad , \quad s_4=-\,a^* \tag{27}$$

It is clear that the roots s_1, s_2, s_3, s_4 satisfy the property that $s_2=-s_1$, $s_4=-s_3$. Here the roots s_1 , s_2 are complex and the roots s_3 , s_4 being real and hence, the principle terms in the series solution (24) have the following type $\begin{pmatrix} A_0 \\ B_0 \end{pmatrix}R^s=\begin{pmatrix} A_0 \\ B_0 \end{pmatrix}R^{s_R+i\,s_I}=\begin{pmatrix} A_0 \\ B_0 \end{pmatrix}R^{s_R}\left\{\cos(s_I\ log\ R\ )+i\ \sin(s_I\ log\ R\ )\right\}$.

Due to Neuringer [50], the dealing of complex case is unlikely the development that the differential equation is needed to solve once previously rather than twice in later. This is relevant to point out that without non-locality effect, viscosity, and thermal effects, i.e. $\xi_0=0$, $\hat{\alpha}_0=0=\hat{\alpha}_1$ and $\tau_q=\tau_T=\tau_\upsilon=0$ which implies that $\tilde{\tau}_q=\tilde{\tau}_T=\tilde{\tau}_\upsilon=\tilde{\alpha}_0=\tilde{\alpha}_1=\tilde{\delta}_0=i\,\Omega^{-1}$. Consequently, all the roots s_1 , s_2 , s_3 , s_4 of the indicial equation turn into real. For indicial roots, the Eq. (26) directs us to write

$$A_0\left(s_j\right)=\begin{cases}1\ ,\ j=1\ ,\ 2\\ 0\ ,\ j=3\ ,\ 4\end{cases}\ ,\ B_0\left(s_j\right)=\begin{cases}0\ ,\ j=1\ ,\ 2\\ 1\ ,\ j=3\ ,\ 4\end{cases} \tag{28}$$

Again, by taking the coefficient of next lower degree term equal to zero i.e. R^{s-1} in Eq. (25), and on simplification we obtain

$$\begin{pmatrix} A_1(s_j) \\ B_1(s_j) \end{pmatrix}=-\begin{pmatrix} 0 & D_{12}^1(s_j) \\ D_{21}^1(s_j) & 0 \end{pmatrix}\begin{pmatrix} A_0(s_j) \\ B_0(s_j) \end{pmatrix} \tag{29}$$

where the values of $D_{12}^1(s_j)$ and $D_{21}^1(s_j)$ are defined in Appendix (A.1).

Similarly, by taking the powers of R^{s+k} equal to zero, Eq. (25) gives the recurrence relation for $\left(A_k(s_j)\quad B_k(s_j)\right)'$; $(k=1\ ,\ 2\ ,\ 3,...)$ and therefore, we can write

$$\begin{pmatrix} A_{k+2}(s_j) \\ B_{k+2}(s_j) \end{pmatrix}=-\begin{pmatrix} 0 & G_{12}^k(s_j) \\ G_{21}^k(s_j) & 0 \end{pmatrix}\begin{pmatrix} A_{k+1}(s_j) \\ B_{k+1}(s_j) \end{pmatrix}-\begin{pmatrix} G_{11}^k(s_j) & 0 \\ 0 & G_{22}^k(s_j) \end{pmatrix}\begin{pmatrix} A_k(s_j) \\ B_k(s_j) \end{pmatrix} \tag{30}$$

where the values of $G_{11}^k(s_j), G_{12}^k(s_j), G_{21}^k(s_j), G_{22}^k(s_j)$ are given in Appendix (A.2).

For $k=0$, the Eq. (30) can be written as:

$$\begin{pmatrix} A_2(s_j) \\ B_2(s_j) \end{pmatrix}=\begin{pmatrix} D_{11}^2(s_j) & 0 \\ 0 & D_{22}^2(s_j) \end{pmatrix}\begin{pmatrix} A_0(s_j) \\ B_0(s_j) \end{pmatrix} \tag{31}$$

where the values of $D_{11}^2(s_j)$, $D_{22}^2(s_j)$ are defined in Appendix (A.3).

Likewise, using $k=1$ in Eq. (30) and after simplification, we obtain:

$$\begin{pmatrix} A_3(s_j) \\ B_3(s_j) \end{pmatrix} = -\begin{pmatrix} 0 & D_{12}^3(s_j) \\ D_{21}^3(s_j) & 0 \end{pmatrix}\begin{pmatrix} A_0(s_j) \\ B_0(s_j) \end{pmatrix} \tag{32}$$

where the values of $D_{12}^3(s_j)$ and $D_{21}^3(s_j)$, are defined in Appendix (A.4).

Plugging $k=2$ in Eq. (30), we obtain (after simplification)

$$\begin{pmatrix} A_4(s_j) \\ B_4(s_j) \end{pmatrix} = \begin{pmatrix} D_{11}^4(s_j) & 0 \\ 0 & D_{22}^4(s_j) \end{pmatrix}\begin{pmatrix} A_0(s_j) \\ B_0(s_j) \end{pmatrix} \tag{33}$$

where the values of $D_{11}^4(s_j)$, $D_{22}^4(s_j)$ are defined in Appendix (A.5) and so on. By proceeding in this way, it is verified that the matrices $\begin{pmatrix} D_{11}^{2k}(s_j) & 0 \\ 0 & D_{22}^{2k}(s_j) \end{pmatrix}$ have a similar form to the matrix $\begin{pmatrix} a_{11} & 0 \\ 0 & a_{22} \end{pmatrix}$, and the matrices $\begin{pmatrix} 0 & D_{12}^{2k+1}(s_j) \\ D_{21}^{2k+1}(s_j) & 0 \end{pmatrix}$ are alike to $\begin{pmatrix} 0 & a_{12} \\ a_{21} & 0 \end{pmatrix}$. Hence, in general we have

$$\begin{pmatrix} A_{2k}(s_j) \\ B_{2k}(s_j) \end{pmatrix} = \begin{pmatrix} D_{11}^{2k}(s_j) & 0 \\ 0 & D_{22}^{2k}(s_j) \end{pmatrix}\begin{pmatrix} A_0(s_j) \\ B_0(s_j) \end{pmatrix} \tag{34}$$

$$\begin{pmatrix} A_{2k+1}(s_j) \\ B_{2k+1}(s_j) \end{pmatrix} = \begin{pmatrix} 0 & D_{12}^{2k+1}(s_j) \\ D_{21}^{2k+1}(s_j) & 0 \end{pmatrix}\begin{pmatrix} A_0(s_j) \\ B_0(s_j) \end{pmatrix} \tag{35}$$

where $D_{11}^{2k}(s_j), D_{22}^{2k}(s_j), D_{12}^{2k+1}(s_j), D_{21}^{2k+1}(s_j)$ are defined in Appendix (A.6) and (A.7).

3.4 Convergence analysis

This is to be noticed that the Eqs. (34) and (35), which may also be represented as:

$$\begin{pmatrix} A_{2k}(s_j) \\ A_{2k}(s_j) \end{pmatrix} \approx O\left(\frac{1}{k}\right)\begin{pmatrix} A^* & 0 \\ 0 & -B^* \end{pmatrix}, \begin{pmatrix} A_{2k+1}(s_j) \\ A_{2k+1}(s_j) \end{pmatrix} \approx O\left(\frac{1}{k}\right)\begin{pmatrix} 0 & A^* \\ -B^* & 0 \end{pmatrix} \tag{36}$$

The sequence in matrix $\{Z_k\}$ is convergent in the field which may be real or complex and ($\underset{k\to\infty}{Lim}\ Z_k = Z$) if each of the component k^2 converges. Upon utilizing above-mentioned facts, we find that both the matrices $\left(A_{2k}(s_j) \quad B_{2k}(s_j)\right)' \to 0$ and $\left(A_{2k+1}(s_j) \quad B_{2k+1}(s_j)\right)' \to 0$, when $k \to \infty$ as observed earlier by Cullen [49]. Hence the solution given in Eq. (24) is uniformly convergent. It is observed from the above mentioned discussion that solution (24) may be written in the series solution as:

$$\begin{pmatrix} V(R) \\ \Psi(R) \end{pmatrix} = R^{s_j} \left\{ (I)_{2\times 2} - \begin{pmatrix} 0 & D_{12}^{1}(s_j) \\ D_{21}^{1}(s_j) & 0 \end{pmatrix} R + \begin{pmatrix} D_{11}^{2}(s_j) & 0 \\ 0 & D_{22}^{2}(s_j) \end{pmatrix} R^2 - \ldots \right\} \begin{pmatrix} A_0(s_j) \\ B_0(s_j) \end{pmatrix} \tag{37}$$

The matrices $D_{ij}^{k}(s_j)$, $(i, j = 1,2; k = 1,2,3...)$ have been defined in Appendices (A.6) and (A.7). Hence, the considered and derived sequences and series in Eq. (24) are analytic functions.

3.5 Formal solutions

The general solution in Eq. (16) with the assistance of Eq. (37) via Eq. (21) can be expressed as:

$$V(R,\tau) = \sum_{k=0}^{\infty} \left(\sum_{j=1}^{2} (E_j D_{11}^{2k}(s_j) R^{s_j} - \sum_{j=3}^{4} (E_j D_{12}^{2k+1}(s_j) R^{1+s_j} \right) R^{2k-a^*} \exp(-i\Omega\tau) \tag{38}$$

$$\psi(R,\tau) = \sum_{k=0}^{\infty} \left(-\sum_{j=1}^{2} (E_j D_{21}^{2k+1}(s_j) R^{1+s_j} + \sum_{j=3}^{4} (E_j D_{22}^{2k}(s_j) R^{s_j} \right) R^{2k-a^*} \exp(-i\Omega\tau) \tag{39}$$

where E_1, E_2, E_3, E_4 are the constants to be determined by using boundary conditions. On utilizing solution (38–39), the stress and temperature gradient are given as:

$$\tau_{RR}(R,\tau) = -i\Omega\tilde{\delta}_0 \sum_{k=0}^{\infty} \begin{bmatrix} \sum_{j=1}^{2} E_j \left((2k + s_j + h^*) D_{11}^{2k}(s_j) + c^* R^2 D_{21}^{2k+1}(s_j) \right) \\ -\sum_{j=3}^{4} E_j \left((2k + s_j + d^*) D_{12}^{2k+1}(s_j) + c^* D_{22}^{2k}(s_j) \right) R \end{bmatrix} R^{2k+s_j+a^*} \exp(-i\Omega\tau) \tag{40}$$

$$\frac{d\Psi(R,\tau)}{dR} = \sum_{k=0}^{\infty} \left(-\sum_{j=1}^{2} E_j (2k + s_j + b^*) D_{21}^{2k+1}(s_j) + \sum_{j=3}^{4} E_j (2k + s_j - a^*) R D_{22}^{2k}(s_j) \right) R^{2k-a^*+s_j} \exp(-i\Omega\tau) \tag{41}$$

where $c^* = \frac{\bar{\varepsilon}}{\tilde{\delta}_0}\tilde{\beta}_0$, $h^* = \left(2(1-2\delta^2)\frac{\tilde{\alpha}_0}{\tilde{\delta}_0} - a^* \right)$, $d^* = \left(2(1-2\delta^2)\frac{\tilde{\alpha}_0}{\tilde{\delta}_0} + b^* \right)$.

The displacement, temperature, radial stress, and temperature gradient in Eqs. (38) to (41) form the main solution of the considered problem, which is influenced to the boundaries conditions in Eqs. (9)–(10) for the evaluation of the solution.

3.6 Non-dimensional boundary conditions and frequency equations

In this section, we consider generalized visco thermoelastic nonlocal sphere/disk subjected to non–dimensional traction free, thermal boundary conditions from Eqs. (9) and (10), hence we have following equations

$$-i\Omega\tilde{\delta}_0 R^{-a^*} \left\{ \frac{\partial V}{\partial R} + h^* \frac{w}{R} - \frac{\bar{\varepsilon}}{\tilde{\delta}_0}\tilde{\beta}_0 \Psi \right\} = 0, \quad \frac{\partial \Psi(R,\tau)}{\partial R} = 0, \quad \text{at} \quad R = 1, \ \hbar \tag{42}$$

$$-i\Omega\tilde{\delta}_0 R^{-a^*} \left\{ \frac{\partial V}{\partial R} + h^* \frac{w}{R} - \frac{\bar{\varepsilon}}{\tilde{\delta}_0}\tilde{\beta}_0 \Psi \right\} = 0, \quad \Psi(R,\tau) = 0, \quad \text{at} \quad R = 1, \ \hbar \tag{43}$$

On applying the solutions (38)–(41) to the boundary conditions (42)–(43), the homogeneous algebraic linear equations have been obtained in four unknown parameters i.e. E_1 , E_2 , E_3 , E_4 . For this, a non-trivial solution is required if the determinant of coefficients E_1 , E_2 , E_3 , E_4 vanishes, thus we have the following frequency equations given below separately in two sets:

Set I: For $k = 0$: The frequency equation is derived as:

$$\det(e'_{ij}) = 0 \; ; i \; , j = 1,2,3,4. \tag{44}$$

Case I: The elements of e'_{ij} $;(i \; , j = 1,2,3,4)$ in thermally insulated boundaries are

$$e'_{1j} = ((s_j + h^*) + c^* D^1_{21}(s_j)); j = 1, 2, ; e'_{1j} = -((s_j + b^* + h^*) D^1_{12}(s_j) + c^*) \; ; j = 3,4,$$

$$e'_{2j} = ((s_j + h^*) + c^* \hbar^2 D^1_{21}(s_j)) \; (\hbar)^{s_j - 1 - a^*} \; ; \; j = 1 \; , 2$$

$$e'_{2j} = -\left(s_j + d^*) D^1_{12}(s_j) + c^*\right) (\hbar)^{s_j + 1 + b^*} \; ; \; j = 3 \; , \; 4, \; e'_{3j} = -(s_j + b^*) \; D^1_{21}(s_j) \; ; \; j = 1 \; , \; 2$$

$$e'_{33} = 0 \; , e'_{34} = -2a^*, e'_{4j} = e'_{3j} \; (\hbar)^{s_j - a^*} \; ; j = 1 \; , \; 2; e'_{43} = 0, e'_{44} = -(2a^*)(\hbar)^{-(1+\alpha)}$$

Case II: The elements of e'_{ij} $;(i \; , j = 1,2,3,4)$ in isothermal boundaries are

$$e'_{1j} = (s_j + h^*) \; ; \; j = 1 \; , \; 2 \; ; \; e'_{1j} = -(s_j + b^* + h^*) D^1_{12}(s_j) \; ; j = 3 \; , \; 4$$

$$e'_{2j} = (s_j + h^*)(\hbar)^{s_j - 1 - a^*} \; ; \; j = 1 \; , 2 \; , \; e'_{2j} = -(s_j + d^*) D^1_{12}(s_j) \; (\hbar)^{s_j + 1 + b^*} \; ; j = 3 \; , \; 4,$$

$$e'_{3j} = -D^1_{21}(s_j); \; j = 1 \; , \; 2; e'_{33} = e'_{34} = 1; e'_{4j} = e'_{3j} \; (\hbar)^{s_j + b^*} \; ; j = 1 \; , \; 2 \; ; e'_{4j} = e'_{3j} \; (\hbar)^{s_j - a^*} \; ; j = 3 \; , \; 4$$

Set II: For $k > 0$: The frequency equation is obtained as:

$$\det(e_{ij}) = 0 \; ; i \; , j = 1,2,3,4. \tag{45}$$

Case I: The elements of e_{ij} $;(i \; , j = 1,2,3,4)$ in thermally insulated boundaries are

$$e_{1j} = \left((2k + s_j + h^*) D^{2k}_{11}(s_j) + c^* D^{2k+1}_{21}(s_j)\right) \; ; \; \; j = 1 \; , \; 2$$

$$e_{1j} = -\left((2k + s_j + d^*) D^{2k+1}_{12}(s_j) + c^* D^{2k}_{22}(s_j)\right) \; ; \; j = 3 \; , \; 4$$

$$e_{2j} = \left((2k + s_j + h^*) D^{2k}_{11}(s_j) + c^* \hbar^2 D^{2k+1}_{21}(s_j)\right) (\hbar)^{2k + s_j - a^*} \; ; \; j = 1 \; , \; 2$$

$$e_{2j} = -\left((2k + s_j + d^*) D^{2k+1}_{12}(s_j) + c^* D^{2k}_{22}(s_j)\right) (\hbar)^{2k + s_j + b^*} \; ; \; j = 3 \; , \; 4$$

$$e_{3j} = -(2k + s_j + b^*) D^{2k+1}_{21}(s_j) \; ; \; j = 1 \; , \; 2 \; , \quad e_{3j} = (2k + s_j - a^*) D^{2k}_{22}(s_j) \; ; \; j = 3 \; , \; 4$$

$$e_{4j} = -(2k + s_j + b^*) D^{2k+1}_{21}(s_j) (\hbar)^{2k - a^* + s_j} \; ; \; j = 1 \; , \; 2$$

$$e_{4j} = (2k + s_j - a^*) D^{2k}_{22}(s_j) (\hbar)^{2k + b^* + s_j} \; ; \; j = 3 \; , \; 4$$

Case II: The elements of e_{ij} $;(i \; , j = 1,2,3,4)$ in isothermal boundaries are

$$e_{1j} = (2k + s_j + h^*) D_{11}^{2k}(s_j);\ j = 1,\ 2;\ e_{1j} = -(2k + s_j + d^*) D_{12}^{2k+1}(s_j);\ j = 3,4$$

$$e_{2j} = e_{1j}\,(\hbar)^{2k+s_j-a^*};\ j = 1,\ 2;\ e_{2j} = e_{1j}\,(\hbar)^{2k+s_j+b^*};\ j = 3,4$$

$$e_{3j} = -D_{21}^{2k+1}(s_j);\ j = 1,\ 2,\quad e_{3j} = D_{22}^{2k}(s_j);\ j = 3,\ 4$$

$$e_{4j} = e_{3j}\,(\hbar)^{2k+b^*+s_j};\ j = 1,\ 2;\ e_{4j} = e_{3j}\,(\hbar)^{2k-a^*+s_j};\ j = 3,\ 4$$

The frequency Eqs. (44) and (45) govern the vibration analysis of inhomogeneous visco thermoelastic sphere in the context of nonlocal elasticity with the TPL model.

4 VALIDATION AND DEDUCTION OF RESULTS

4.1 Nonlocal thermoelastic functionally graded sphere/disk

If the viscous effects $(\alpha_0 = 0 = \alpha_1)$ are ignored, so that $\alpha_0 = \tilde{\alpha}_1 = \tilde{\beta}_0 = \tilde{\delta}_0 = i\,\Omega^{-1}$ and $m_2 = 2[\beta(1-\delta^2)-1]$. The above analysis has been transformed to that of generalized nonlocal thermoelastic sphere. However, in the absence of thermal relaxation times $(t_T = t_\nu = t_q = 0)$, $t_q = t_0 > 0$, $K^* = 0$ and nonlocal parameters $\xi_0 = 0$, then the above-mentioned results further reduced to the vibrations of the coupled generalized thermoelastic sphere.

4.2 Nonlocal viscoelastic functionally graded sphere/disk

Here, the thermal equilibrium is set up, then $(\varepsilon_T = 0 = K = T,\ t_T = t_\nu = t_q = 0)$, then this analysis has been reduced to nonlocal viscoelastic hollow sphere. Furthermore, for the case when the viscous effects and the nonlocal parameter in solid is ignored so that $\alpha_0 = 0 = \alpha_1$ and $\xi_0 = 0$, then the analysis has been deduced to elastic sphere/disk which agree from Keles and Tutuncu [28] for the transversely isotropic case.

5 NUMERICAL RESULTS AND DISCUSSIONS

The analytical results have been validated with the help of numerical simulations and computations for stress free thermally insulated and isothermal boundaries of nonlocal TPL visco thermoelastic sphere by applying the iteration method through software like MATLAB. The physical data of material 'polymethyl methacrylate' has been assumed from Othman et al. [20] in Table 1 as follows:

Table 1
Physical data of polymethyl methacrylate material.

S. No	Name of Coefficient	Coefficient	Units	Value
1	Mass density	ρ	$kg\ m^{-3}$	1900
2	Reference Temperature	T_0	K	773
3	Leme's constant	λ	Nm^{-2}	5.16×10^{8}
4	Leme's constant	μ	Nm^{-2}	5.01×10^{8}
5	Thermal Conductivity	K	$W\ m^{-1}K^{-1}$	19.00
6	Coefficient of linear thermal expansion	α_T	K^{-1}	77×10^{-6}
7	Specific heat at constant strain	C_e	$J\,kg^{-1}K^{-1}$	1400
8	Thermoelastic characteristic frequency	ω^*	s^{-1}	1.11×10^{11}
9	Viscoelastic relaxation time	$\hat{\alpha}_0 = \hat{\alpha}_1$		0.05

For the TPL model, the numerical constants has considered as $\tau_v = 1.1$, $\tau_t = 1.3$, $\tau_q = 2.4$ and $K^* = 29.70\, Wm^{-1}K^{-1}$. The non-dimensional value of the nonlocal parameter is taken from Sarkar et al. [19] as $\xi_0 = 2.3102$. The computations have been carried out for Eqs. (45) by considering appropriate values of the Fröbenius parameter $k = 20$, to acquire the frequency Ω. Further, Ω is expressed in the form $\Omega^m = \Omega_R^m + i\,\Omega_I^m$, the non–dimensional frequency (real part) and dissipation factor (imaginary part) which is further written as $f_R = \Omega_R^m$ and $D_I = \Omega_I^m$, here m represent the mode number which gives us the roots of Eq. (45). The computed and simulated thermoelastic damping, frequencies, and frequency shift have been represented graphically for TPL, DPL, GN-III, LS, CTE models of thermoelasticity. The thermoelastic damping and frequency shift have been defined (Sharma et al. [31]) as given below:

$$Q^{-1} = 2\left|\frac{D_I}{f_R}\right|, \quad \Omega_{shift} = \left|\frac{f_R^{Z^*} - f_R^{CTE}}{f_R^{CTE}}\right|$$

Here Z^* denotes for TPL, DPL, GN–III materials and CTE stand for coupled thermoelasticity. Because of the domain of the problem i.e. $1 \le x \le \hbar$, we have fixed the inner radius at $\hbar = 1.0$ and thereafter, computations have been taken for ratio of outer to inner radii i.e. $\hbar = 2.0$ and $\hbar = 4.0$.

Figs.1(a) to 1(b) have been presented for natural frequencies (f_n) (i.e. real part of Ω) versus the mode number (m) for ratio of outer to inner radius i.e. $\hbar = 2.0$ by considering thermally insulated and isothermal boundaries of the generalized nonlocal visco thermoelastic sphere/disk. These figures depict that as the value of mode number (m) increases, the variation of vibrations also increases. However, a decreasing trend of variation of frequencies is observed as the values of grading index parameter varies form $\alpha = -3.5$ to $\alpha = +3.5$.

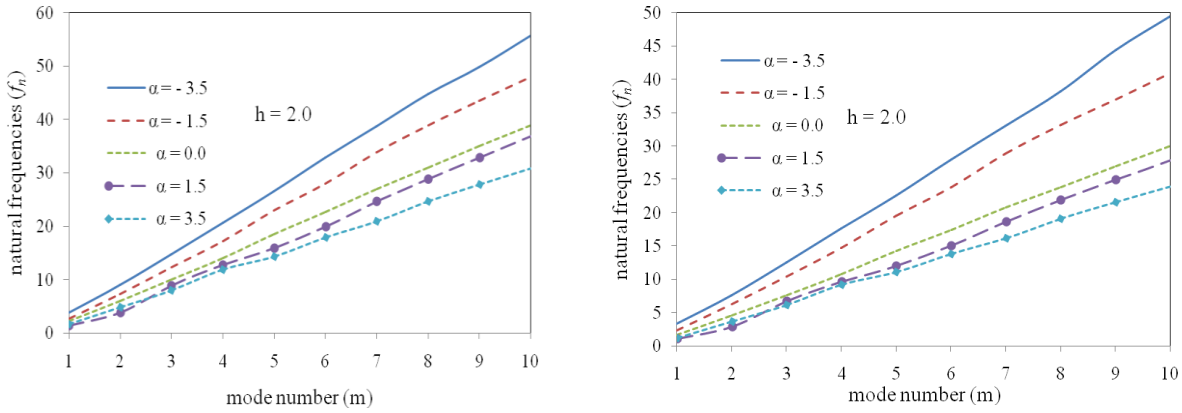

Fig.1
Natural frequencies (f_n) against mode number (m) for different values of grading index (α) at $\hbar = 2.0$ for (a) thermally insulated (b) isothermal boundaries.

Figs. 2(a) to 2(b) and Figs. 3(a)-3(b) have been shown for thermoelastic damping (Q^{-1}) versus grading index (α) for TPL, DPL, GN–III, LS, and CTE theories of generalized thermoelasticity for the material (nonlocal) at outer to inner radial ratios $\hbar = 2.0$ and $\hbar = 4.0$ respectively. It is observed from Fig. 2(a) that in initial stage, there is a high variation at $\alpha = -5.0$ for TPL, DPL, and GN–III theories of generalized thermoelasticity rather than LS and CTE theories of thermoelasticity for the thickness $\hbar = 2.0$. As the value of α increases, the vibrations show sinusoidal behavior and go on decreasing having variation of peaks at $\alpha = -3.0, -2.0, 0.0, 1.0, 2.0$ after that the vibrations die out. This is also observed from Fig. 2(b) that initially there is high variation at $\alpha = -5.0$ and,

as α increases, the variation of vibrations show sinusoidal behavior and the vibrations achieve maximum variation at $\alpha = 0.0$, 2.0, then go on decreasing for the thickness $\hbar = 2.0$. Fig. 3(a) which has been presented for the thickness $\hbar = 4.0$ depicts that initially there is high variation at $\alpha = -5.0$, and as α increases, the variations go on decreasing with peaking at $\alpha = -3.0, -2.0, -1.0, 0.0$ achieve maximum variation and die out. It is observed from Fig. 3(b) that the peaks are to be noticed at $\alpha = -4.0, -3.0, -2.0, -1.0, 0.0,$ and as α increases; the vibrations began to decrease and become asymptotic at $\alpha = 3.0$ for thickness $\hbar = 4.0$. It is to be noticed from Figs. 2(a)-2(b) and Figs. 3(a) to 3(b) that in the case of TPL model the variations are higher as compared to DPL, GN–III, LS and CTE.

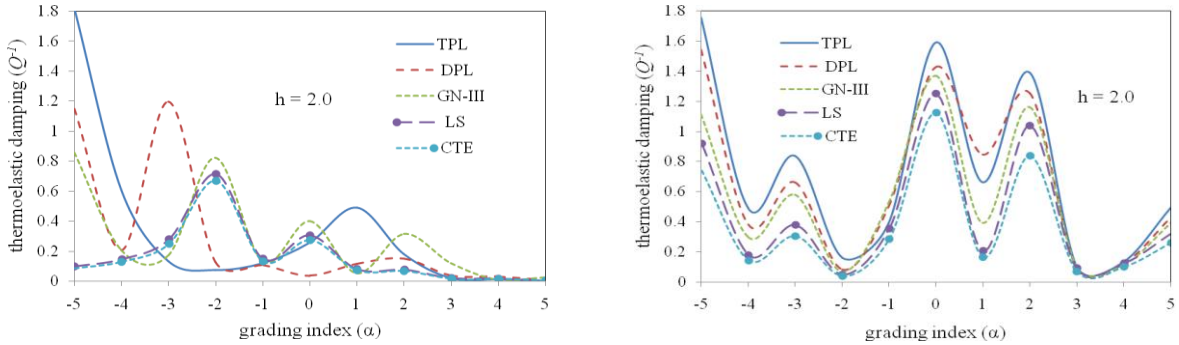

Fig.2
Comparison of thermoelastic damping (Q^{-1}) against grading index (α) between theories of thermoelasticity at $\hbar = 2.0$ for (a) thermally insulated (b) isothermal boundaries.

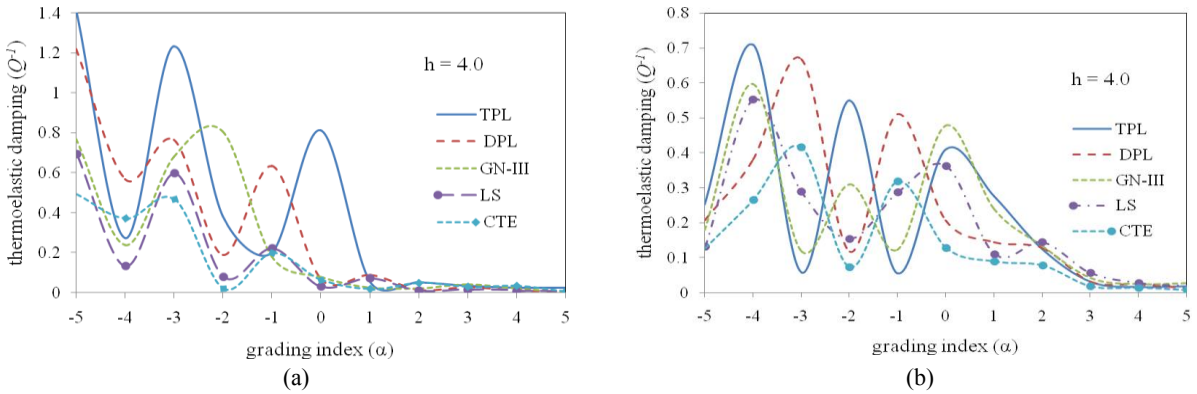

Fig.3
Comparison of thermoelastic damping (Q^{-1}) against grading index (α) between theories of thermoelasticity at $\hbar = 4.0$ for (a) thermally insulated (b) isothermal boundaries.

Fig. 4(a) and Fig. 5(a) have been between thermoelastic damping and mode number for $\alpha = -1.5$, 0.0, 1.5 with the comparison of local to nonlocal elastic materials at $\hbar = 2.0$, 4.0 for thermally insulated boundaries. Fig. 4(a) and Fig. 5(a) depict that the variation of damping at $\alpha = -1.5$, 0.0 for both the local as well as nonlocal cases show higher variations initially, and as m increases, the vibrations achieve maximum amplitude at $m = 4.0$ and $m = 2.0$ and go on decreasing with sinusoidal behavior. The thermoelastic damping for the comparison of local and nonlocal cases at $\alpha = 1.5$, the vibrations show larger variations and with a further increase in the mode number (m), the vibrations go on decreasing with sinusoidal behavior. It has been noticed from Fig. 5(a) that for $\alpha = 0.0, 1.5$ the variations achieves maximum variations between $4.0 \le m \le 6.0$. Fig. 4(b) and Fig. 5(b) have been presented for thermoelastic damping (Q^{-1}) against m for different values of grading index with a comparison of nonlocal to local elastic materials with thickness $\hbar = 2.0$, 4.0 for isothermal boundary conditions.

Fig. 4(b) and Fig. 5(b) represent the variation of thermoelastic damping at $\alpha = -1.5$, $0.0, \alpha = 1.5$ for nonlocal and local cases, the figures show low variations initially, and as the value of mode number increase, the variations acquired more or less amplitudes at $m = 2.0$, 4.0 , 5.0 , 7.0 , further go on decreasing. It has been observed from the Figs. 4(a)-4(b) and Figs. 5(a)-5(b) that the variations are slightly larger for the nonlocal case in contrast to local case.

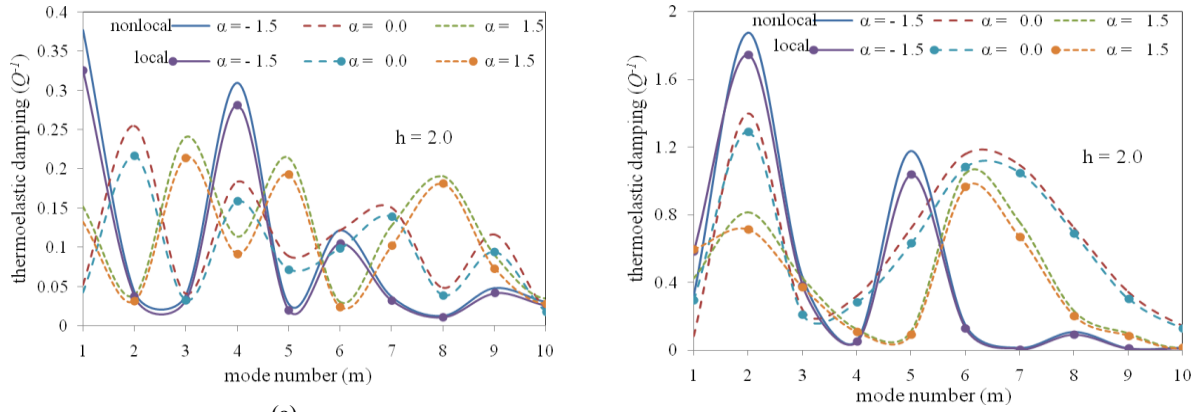

Fig.4

Comparison between nonlocal and local thermoelastic damping (Q^{-1}) against mode number (m) for different values of grading index (α) at $\hbar = 2.0$ for (a) thermally insulated (b) isothermal boundaries.

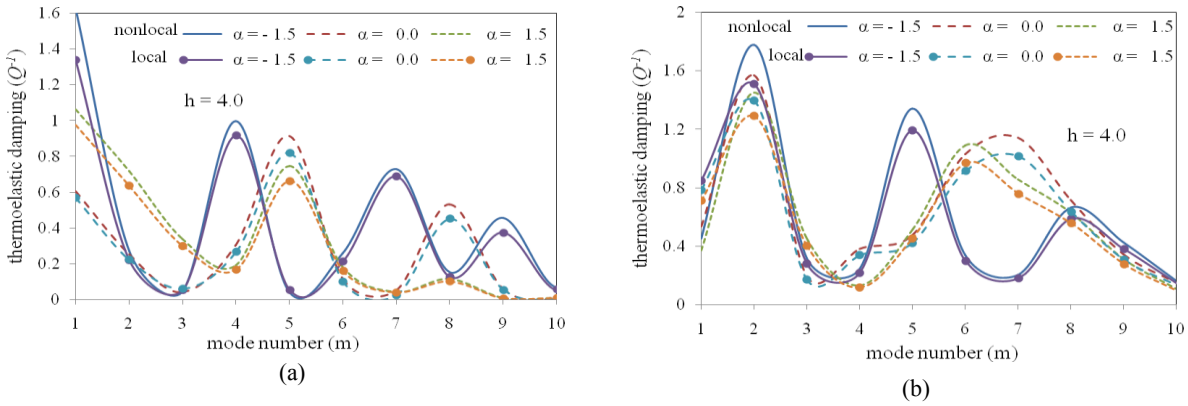

Fig.5

Comparison between nonlocal and local thermoelastic damping (Q^{-1}) against mode number (m) for different values of grading index (α) at $\hbar = 4.0$ for (a) thermally insulated (b) isothermal boundaries.

Figs. 6(a)-6(b) have been presented for homogenous material $\alpha = 0.0$ when $\hbar = 2.0$ by considering the thermally insulated and isothermal boundaries. It is revealed from Fig. 6(a) that the behavior of frequency shift (Ω_{shift}) displays high vibrations for the nonlocal case in comparison to the local elastic case. It is also observed that variations are high initially and with an increase in values of m, it decreases up to $m = 3.0$, increases slightly between $4.0 \le m \le 5.0$, and further go on decreasing. The Fig. 6 (b) depicts that for the TPL case, the variation increases, achieve peak value at $m = 7.0$ and then go on decreasing. For the cases of DPL and GN–III, the maximum amplitude of variation has been observed at $m = 5.0$ and goes on decreasing as the value of m increases. Figs. 7(a) and 7(b) have been represented for inhomogeneous material $\alpha = 2.5$ when thickness $\hbar = 2.0$. It is revealed from Fig. 7(a), that for all generalized theories TPL, DPL, and GN–III, a variation of frequency shift shows the peak value between $5.0 \le m \le 7.0$ for the both nonlocal and local elastic materials. Fig. 7(b) depicts that the

variations are low when $m=1$, achieve maximum variation when $6.0 \le m \le 8.0$ for TPL case, sinusoidal behavior for DPL and GN–III; and the vibrations began to decrease as the value of *m* increases. In a comparison of the above figures, the variations of frequency shift follow the inequality $\Omega_{TPL} > \Omega_{DPL} > \Omega_{GN-III}$ for Fig. 6 and follow the inequality $\Omega_{TPL} < \Omega_{DPL} < \Omega_{GN-III}$ for Fig. 7. These inequalities clearly depict the impact of in-homogeneity for both nonlocal as well as local elastic materials.

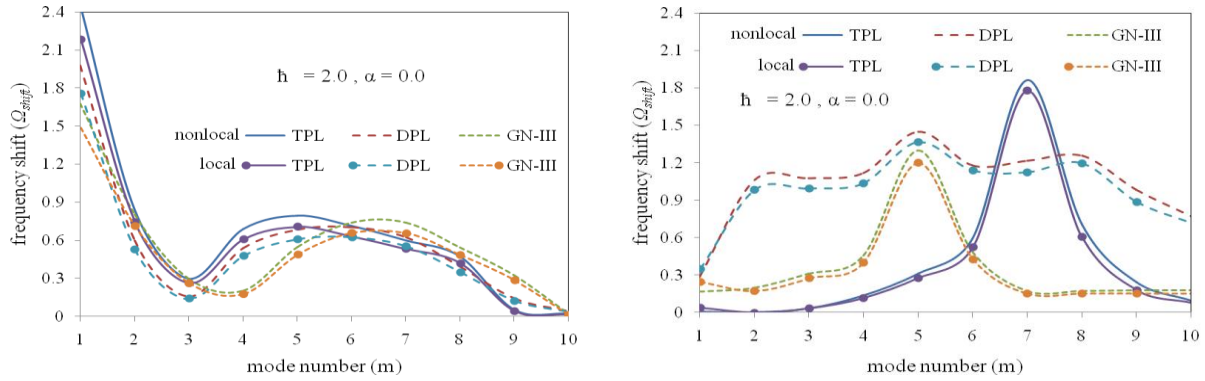

Fig.6
Comparison between nonlocal and local frequency shift (Ω_{shift}) against mode number (m) for TPL, DPL and GN–III at $\hbar = 2.0,\ \alpha = 0.0$ for (a) thermally insulated (b) isothermal boundaries.

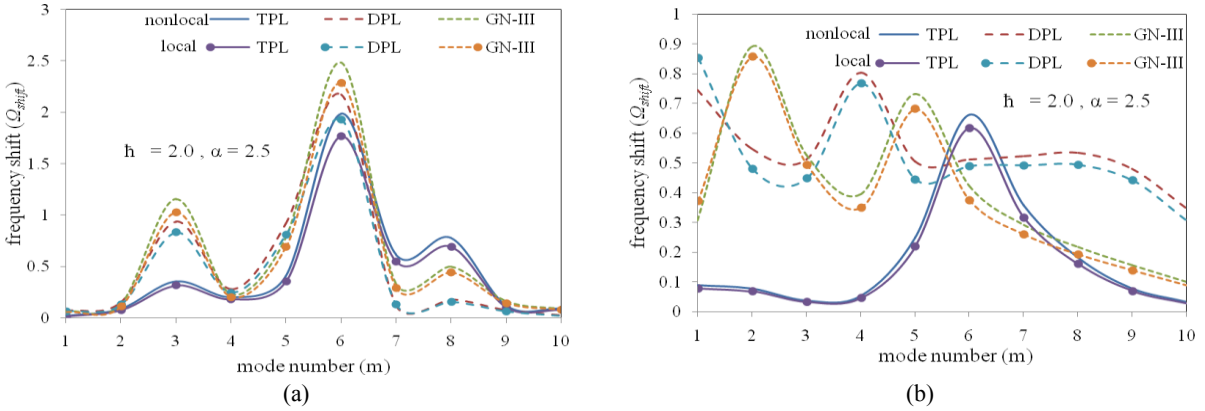

Fig.7
Comparison between nonlocal and local frequency shift (Ω_{shift}) against mode number (m) for TPL, DPL and GN–III at $\hbar = 2.0,\ \alpha = 2.5$ for (a) thermally insulated (b) isothermal boundaries.

Because of the change in thermal boundary conditions, the frequency shift is derived as $\Omega B_{shift} = \left| \left((\Omega_R^m)_{(ins)} - (\Omega_R^m)_{(iso)} \right) \Big/ (\Omega_R^m)_{(iso)} \right|$, here $(\Omega_R^m)_{(ins)}$ represents the frequencies for thermally insulated conditions and $(\Omega_R^m)_{(iso)}$ stands for the natural frequencies for isothermal boundary conditions. Frequency shift have been presented in Figs. 8(a)–8(b) for thermally insulated to isothermal boundaries as a function of *m* (mode number) for theories of generalized thermoelasticity i.e. TPL, DPL, GN–III. This is to be observed from Fig. 8(a) (illustrated for homogenous case i.e. $\hbar = 2.0$, $\alpha = 0.0$) that the vibrations are high initially for all the generalized theories, achieve maximum variation when $m = 3.0$ and $m = 5.0$, further the vibrations began to decrease. It is observed from Fig. 8(b) (illustrated for inhomogeneous case, i.e. $\hbar = 2.0$, $\alpha = 2.5$) that the vibrations are low initially when $m = 1$ for all the theories, achieve low peaks at $m = 3.0$ and high peak at $m = 6.0$ for all models i.e. TPL, DPL, GN–III; therefore, as the values of *m* increases, the variation of vibrations began to decrease. It has been observed from Figs. 8(a) and 8(b) that the variations in Fig. 8(a) obeys the inequality $TPL > DPL > GN-III$ and also

the variations of peaks at $m = 6.0$ in Fig. 8(b) obeys the trends of inequality $GN - III > DPL > TPL$ because of the inhomogeneity.

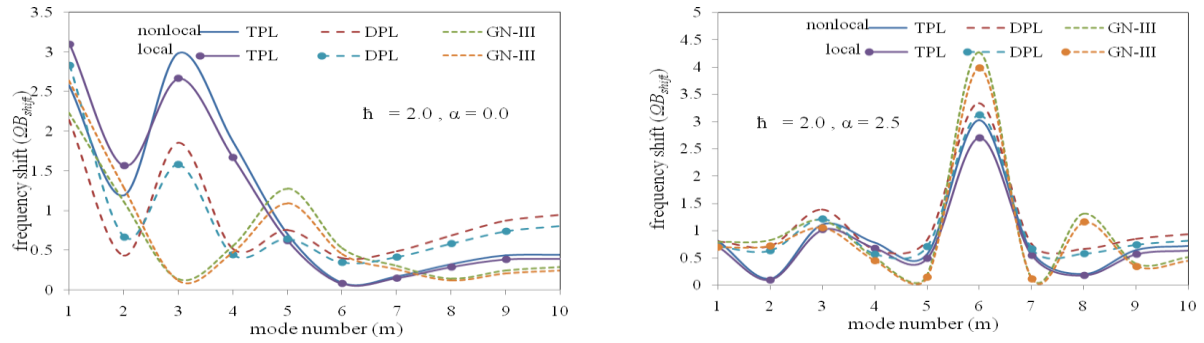

Fig.8
Comparison between nonlocal and local thermally insulated to isothermal frequency shift (ΩB_{shift}) against mode number (m) for TPL, DPL, GN–III at (a) homogenous material i.e. $\hbar = 2.0, \alpha = 0.0$. (b) in–homogenous material i.e. $\hbar = 2.0, \alpha = 2.5$.

6 CONCLUSIONS

The inhomogeneous visco thermoelastic nonlocal elastic hollow spheres in radial direction have been studied in the reference of TPL model of generalized thermoelasticity. Based on the non-locality effect, the Fröbenius method has been considered to solve the differential equations. Frequency equations have been solved for stress-free boundary conditions to check the behavior of frequencies for the local and nonlocal elastic materials. Some general concluding remarks and remedies have been listed as below:

1. The Fröbenius method for the models of generalized thermoelasticity i.e. TPL, DPL, GN–III, LS and CTE in nonlocal elasticity has been effectively applied to investigate axisymmetric vibrations of generalized three-phase-lag model of visco thermoelastic spheres.
2. The TPL model has been inferred for thermoelastic, nonlocal elastic and viscoelastic spheres.
3. Frequency shift and the thermoelastic damping linked to quality factor can be monitored with the grading index to improve the signals of quality of the modes of vibrations.
4. With the facilitation of inhomogeneity parameter i.e. grading index, the loss of energy may be optimized.
5. The thermal relaxation times for generalized theories of thermoelasticity and thermoelastic coupling parameters have important effects on the characteristics and vibrations, like frequency shift and damping.
6. This is to be noticed from the behavior of every graphical figure that the variations are maximum for the extreme negative value of grading index and minimum for the extreme positive value of grading index. Hence obey the trends of inequality for $\alpha \in (-3.5 > 1.5 > 0.0 > 1.5 > 3.5)$ which pointed out inhomogeneity effect for local and nonlocal elastic materials.

APPENDIX

$$D_{12}^{1}(s_j) = \frac{A^*(s_j + b^* + 1)}{(s_j + 1)^2 - n^2}, \quad D_{21}^{1}(s_j) = \frac{-B^*(s_j + b^* + 2)}{(s_j + 1)^2 - (a^*)^2} \tag{A.1}$$

$$\left.\begin{aligned} G_{11}^{k}(s_j) &= \frac{i\Omega}{\tilde{\delta}_0^* \left\{(s_j + k + 2)^2 - n^2\right\}}, \quad G_{12}^{k}(s_j) = \frac{A^*\left(s_j + k + 1 + b^*\right)}{(s_j + k + 2)^2 - n^2}, \\ G_{21}^{k}(s_j) &= \frac{-B^*\left(s_j + k + 2 + b^*\right)}{(s_j + k + 2)^2 - (a^*)^2}, \quad G_{22}^{k}(s_j) = \frac{\Omega^*\Omega^2\tilde{\tau}_q}{(s_j + k + 2)^2 - (a^*)^2}, \end{aligned}\right\} (k = 1, 2, 3, \ldots). \tag{A.2}$$

$$\begin{cases} D_{11}^{2}(s_j) = \left\{ G_{12}^{0}(s_j) D_{21}^{1}(s_j) - G_{11}^{0}(s_j) \right\} \\ D_{22}^{2}(s_j) = \left\{ G_{21}^{0}(s_j) D_{12}^{1}(s_j) - G_{22}^{0}(s_j) \right\} \end{cases}. \tag{A.3}$$

$$\begin{cases} d_{12}^{3}(s_j) = \left\{ -G_{12}^{1}(s_j) D_{22}^{2}(s_j) + G_{11}^{2}(s_j) D_{12}^{1}(s_j) \right\}, \\ d_{21}^{3}(s_j) = \left\{ -G_{21}^{1}(s_j) D_{11}^{2}(s_j) + G_{22}^{1}(s_j) D_{21}^{1}(s_j) \right\}. \end{cases} \tag{A.4}$$

$$\begin{cases} d_{11}^{4}(s_j) = \left\{ G_{12}^{2}(s_j) D_{21}^{3}(s_j) - G_{11}^{2}(s_j) D_{11}^{2}(s_j) \right\}, \\ d_{22}^{4}(s_j) = \left\{ G_{21}^{2}(s_j) D_{12}^{3}(s_j) - G_{22}^{2}(s_j) D_{22}^{2}(s_j) \right\}, \end{cases} \tag{A.5}$$

$$\begin{cases} D_{11}^{2k}(s_j) = (G_{12}^{2k-2}(s_j) D_{21}^{2k-1}(s_j) - G_{11}^{2k-2}(s_j) D_{11}^{2k-2}(s_j)), \\ D_{22}^{2k}(s_j) = (G_{21}^{2k-2}(s_j) D_{12}^{2k-1}(s_j) - G_{22}^{2k-2}(s_j) D_{22}^{2k-2}(s_j)), \\ D_{12}^{2k+1}(s_j) = (-G_{12}^{2k-1}(s_j) D_{22}^{2k}(s_j) + G_{11}^{2k-1}(s_j) D_{12}^{2k-1}(s_j)), \\ D_{21}^{2k+1}(p_j) = (-G_{21}^{2k-1}(s_j) D_{11}^{2k}(s_j) + G_{22}^{2k-1}(s_j) D_{21}^{2k-1}(s_j)), \end{cases} \quad (k = 1, 2, 3 \ldots) \tag{A.6}$$

with

$$\begin{pmatrix} D_{11}^{0}(s_j) & D_{12}^{0}(s_j) \\ D_{21}^{0}(s_j) & D_{22}^{0}(s_j) \end{pmatrix} = \begin{pmatrix} 1 & 0 \\ 0 & 1 \end{pmatrix} \quad (j = 1, 2, 3, 4) \tag{A.7}$$

REFERENCES

[1] Nowacki W., 1975, *Dynamic Problems of Thermoelasticity*, Noordhof, Leyden, The Netherlands.

[2] Lord H.W., Shulman Y., 1967, Generalized dynamical theory of thermoelasticity, *Journal of the Mechanics and Physics of Solids* **15**: 299-309.

[3] Green A.E., Lindsay K.A., 1972, Thermoelasticity, *Journal of Elasticity* **2**: 1-7.

[4] Green A.E., Naghdi P.M., 1993, On thermoelasticity without Energy Dissipation, *Journal of Elasticity* **31**: 189-208.

[5] Chandrasekharaiah D.S., 1998, Hyperbolic thermoelasticity: A review of recent literature, *Applied Mechanics Reviews* **51**: 705-729.

[6] Tzou D.Y., 1995, A unified field approach for heat conduction from macro to micro-scales, *ASME Journal of Heat Transfer* **117**: 8-16.

[7] Choudhuri S.R., 2007, On a thermoelastic three-phase-lag model, *Journal of Thermal Stresses* **30**: 231-238.

[8] Biswas S., Mukhopadhyay B., 2018, Rayleigh surface wave propagation in transversely isotropic medium with three-phase-lag model, *Journal of Solid Mechanics* **10**(1): 175-185.

[9] Quintanilla R., 2009, A well-posed problem for the three-dual-phase-lag heat conduction, *The Journal of Thermal Stresses* **32**: 1270-1278.

[10] Sharma D.K., Bachher M., Sarkar N., 2020, Effect of phase-lags on the transient waves in an axisymmetric functionally graded visco thermoelastic spherical cavity in radial direction, *International Journal of Dynamics and Control* DOI: 10.1007/s40435-020-00659-2.

[11] Eringen A.C., 2002, *Nonlocal Continuum Field Theories*, Springer Verlag, New York.

[12] Ghadiri M., Shafiei, N., Hossein Alavi S., 2017, Vibration analysis of a rotating nanoplate using nonlocal elasticity theory, *Journal of Solid Mechanics* **9**(2): 319-337.

[13] Li C., Tian X., He T., 2020, Nonlocal thermo-viscoelasticity and its application in size-dependent responses of bi-layered composite viscoelastic nano-plate under non uniform temperature for vibration control, *Mechanics of Advanced Materials and Structures* Doi:10.1080/15376494.2019.1709674.

[14] Zarei M., Ghalami-Choobar M., Rahimi, G.H., Faghani, G.R., 2018, Free vibration analysis of non-uniform circular nanoplate, *Journal of Solid Mechanics* **10**(2): 400-415.

[15] Najafizadeh M.M., Raki M., Yousefi P., 2018, Vibration analysis of FG nanoplate based on third-order shear deformation theory (TSDT) and nonlocal elasticity, *Journal of Solid Mechanics* **10**(3): 464-475.

[16] Bachher M., Sarkar N., 2019, Nonlocal theory of thermoelastic materials with voids and fractional derivative heat transfer, *Waves in Random and Complex Media* **29**: 595-613.
[17] Mondal S., Sarkar N., Sarkar N., 2019, Waves in dual-phase-lag thermoelastic materials with voids based on Eringen's nonlocal elasticity, *The Journal of Thermal Stresses* **42**: 1035-1050.
[18] Asbaghian Namin S.F., Pilafkan R., 2018, Influences of small-scale effect and boundary conditions on the free vibration of nano-plates: A molecular dynamics simulation, *Journal of Solid Mechanics* **10**(3): 489-501.
[19] Sarkar N., De S., Sarkar N., 2019, Waves in nonlocal thermoelastic solids of type II, *The Journal of Thermal Stresses* **42**: 1153-1170.
[20] Othman M.I.A., Ezzat M.A., Zaki S.A., El-Karamany A.S., 2002, Generalized thermo-viscoelastic plane waves with two relaxation times, *International Journal of Engineering Science* **40**: 1329-1347.
[21] Othman M.I.A., Hasona W.M., Mansour N.T., 2015, The effect of Magnetic field on generalized thermoelastic medium with two temperature under three–phase–lag Model, *Multidiscipline Modeling in Materials and Structures* **11**(4): 544-557.
[22] Soltani P., Bahramian R., Saberian, J., 2015, Nonlinear vibration analysis of the fluid-filled single walled carbon nanotube with the shell model based on the nonlocal elacticity theory, *Journal of Solid Mechanics* **7**(1):58-70.
[23] Marin M., Craciun E-M., Pop N., 2016, Consideration on mixed initial-boundary value problems for micropolar porous bodies, *Dynamic System and Applications* **25**: 175-196.
[24] Lamb H., 1881, On the vibrations of an elastic sphere, *Proceedings of the London Mathematical Society* **13**: 189-212.
[25] Sato Y., Usami T., 1962, Basic study on the oscillation of homogeneous elastic sphere; Part I, Frequency of the free oscillations, *Geophysics Magazine* **31**: 15-24.
[26] Sato Y., Usami T., 1962, Basic study on the oscillation of a homogeneous elastic sphere; Part II, Distribution of displacement, *Geophysics Magazine* **31**: 25-47.
[27] Hsu M.H., 2007, Vibration Analysis of Annular Plates, *Tamkang Journal of Science and Engineering* **10**(3): 193-199.
[28] Keles I., Tutuncu N., 2011, Exact analysis of axisymmetric dynamic response of functionally graded Cylinders (or disks) and Spheres, *Journal of Applied Mechanics* **78**: 061014.
[29] Sharma J.N., Sharma D. K., Dhaliwal S.S., 2012, Three-dimensional free vibration analysis of a visco thermoelastic hollow sphere, *Open Journal of Acoustics* **2**: 12-24.
[30] Sharma J.N., Sharma D. K., Dhaliwal S.S., 2013, Free vibration analysis of a rigidly fixed visco thermoelastic hollow sphere, *Indian Journal of Pure and Applied Mathematics* **44**: 559-586.
[31] Sharma D.K., Sharma J.N., Dhaliwal S.S., Walia V., 2014, Vibration analysis of axisymmetric functionally graded visco thermoelastic spheres, *Acta Mechanica Sinica* **30**: 100-111.
[32] Nejad M.Z., Rastgoo A., Hadi A., 2014, Effect of exponentially-varying properties on displacements and stresses in pressurized functionally graded thick spherical shells with using iterative technique, *Journal of Solid Mechanics* **6**(4):366-377.
[33] Sharma D.K., 2016, Free vibrations of homogenous isotropic visco thermoelastic spherical curved plates, *Journal of Applied Science and Engineering* **19**(2): 135-148.
[34] Biswas S., Mukhopadhyay B., 2019, Three-dimensional vibration analysis in transversely isotropic cylinder with matrix frobenius method, *The Journal of Thermal Stresses* **42**(10):1207-1228.
[35] Biswas S., 2019, Eigenvalue approach to a magneto-thermoelastic problem in transversely isotropic hollow cylinder: comparison of three theories, *Waves in Random and Complex Media* Doi:10.1080/17455030.2019.1588484.
[36] Sharma D. K., Sharma S. R., Walia V., 2018, Analysis of axisymmetric functionally graded forced vibrations due to heat sources in visco thermoelastic hollow sphere using series solution, *AIP Conference Proceedings* **1975**: 030010.
[37] Sharma D.K., Mittal H., Sharma S.R., 2019, Forced vibration analysis in axisymmetric functionally graded visco thermoelastic hollow cylinder under dynamic pressure, *Proceedings of the National Academy of Sciences, India Section A: Physical Sciences*.
[38] Manthena V.R., Lamba N.K., Kedar G.D., 2018, Mathematical modeling of thermoelastic state of a thick hollow cylinder with nonhomogeneous material properties, *Journal of Solid Mechanics* **10**(1): 142-156.
[39] Manthena V.R., Lamba N.K., Kedar G.D., 2018, Estimation of thermoelastic state of a thermally sensitive functionally graded thick hollow cylinder: A mathematical model, *Journal of Solid Mechanics* **10**(4): 766-778.
[40] Sharma D.K., Mittal H., 2019, Analysis of free vibrations of axisymmetric functionally graded generalized visco thermoelastic cylinder using series solution, *Journal of Vibration Engineering & Technologies* DOI: 10.1007/s42417-019-00178-1.
[41] Riaz A., Ellahi, R., Bhatti M.M., Marin M., 2019, Study of heat and mass transfer in the Eyring–Powell model of fluid propagating peristaltically through a rectangular compliant channel, *Heat Transfer Research* **50**(16): 1539-1560.
[42] Bhatti M.M., Ellahi R., Zeeshan A., Marin M., Ijaz N., 2019, Numerical study of heat transfer and Hall current impact on peristaltic propulsion of particle-fluid suspension with compliant wall properties, *Modern Physics Letters B* **33**(35): 1950439.
[43] Sharma D.K., Thakur P.C., Sarkar N., Bachher, M., 2020, Vibrations of a nonlocal thermoelastic cylinder with void, *Acta Mechanica* **231**: 2931-2945.
[44] Sharma D.K., Thakur D., Walia V., Sarkar N., 2020, Free vibration analysis of a nonlocal thermoelastic hollow cylinder with diffusion, *The Journal of Thermal Stresses* **43**(8): 981-997.

[45] Biswas S., 2020, Fundamental solution of steady oscillations equations in nonlocal thermoelastic medium with voids, *The Journal of Thermal Stresses* **43**(3): 284-304.
[46] Pramanik A.S., Biswas S., 2020, Surface waves in nonlocal thermoelastic medium with state space approach, *The Journal of Thermal Stresses* **43**(6): 667-686.
[47] Noda N., Jin Z. H., 1993, Thermal stress intensity factor for a crack in a strip of functionally graded material, *International Journal of Solids and Structures* **30**: 1039-1056.
[48] Tomantschger K.W. 2002, Series solutions of coupled differential equations with one regular singular point, *Journal of Computational and Applied Mathematics* **140**: 773-783.
[49] Cullen C.G., 1972, *Matrices and Linear Transformation*, Addison–Wesley Pub., Reading Massachusetts.
[50] Neuringer J.L., 1978, The Fröbenius method for complex roots of the indicial equation, *International Journal of Mathematical Education in Science and Technology* **9**: 71-77.